

Thermal Conductivity of Propane in the Temperature Range 25–305°C and Pressure Range 1–70 MPa

R. Tufeu¹ and B. Le Neindre¹

Received January 28, 1986

A coaxial cylinder method was used to measure the thermal conductivity of propane in the pressure range from 1 to about 70 MPa and in the temperature range from room temperature to 305°C. The behavior of the thermal conductivity in the critical region was carefully investigated.

KEY WORDS: critical region; high pressure; propane; thermal conductivity.

1. INTRODUCTION

Up to now, the most significant measurements of the thermal conductivity of propane were made by Leng and Comings [1], Ryabtsev and Kazaryan [2], Carmichael et al. [3], Brykov et al. [4], and more recently at lower temperatures by Roder and Nieto de Castro [5]. Tentative tables and correlations representing the thermal conductivity of propane as a function of temperature and pressure (or density) have been reported [6, 7], but it has been pointed out that the set of data used to generate these tables should be improved, especially in the critical region, where almost no data exist. Thus, new measurements of the thermal conductivity of propane were performed over wide temperature and pressure ranges (25–305°C and up to 70 MPa); special attention was paid to the critical region.

These measurements are a part of an extensive program carried on in our laboratory to determine the thermal conductivity of hydrocarbons. The thermal conductivities of methane [8, 9], ethane [9, 10], *n*-butane [11], and isobutane [12] are already available.

¹ Laboratoire des Interactions Moléculaires et des Hautes Pressions–CNRS, Université Paris-Nord, Avenue J. B. Clément, 93430 Villetaneuse, France.

2. EXPERIMENTAL METHOD

The thermal conductivity was measured with a concentric cylinder apparatus described in earlier publications [13, 14]. The experimental procedure was identical to that used, for example, in measuring the thermal conductivity of *n*-butane [11]. The fluid is located in the annular gap between two coaxial cylinders with the axis in the vertical direction. The thermal conductivity was determined by measuring the temperature difference between the inner and the outer cylinders as a function of the energy dissipated from the inner cylinder. The temperature difference between the two cylinders varies from 0.3°C close to the critical point to about 2°C far away from the critical point; this temperature difference was measured with an accuracy of approximately $\pm 0.003^\circ\text{C}$. The temperature was measured with an accuracy of $\pm 0.02^\circ\text{C}$, and the pressure with an accuracy of 0.1%.

To determine the thermal conductivity, we need to consider the corrections due to heat transferred by radiation, spurious heat flow from the inner to the outer cylinder through the solid centering pins and the wires, heat transferred by convection, and the effects of a possible temperature jump at the boundaries of the fluid layer and surfaces of the cylinders [14].

We calculated the radiation correction from the Stefan–Boltzmann radiation law, assuming that the absorption of radiation by the fluid could be neglected.

The correction for heat losses through the solid parts of the cell was determined from a set of calibration measurements with argon, neon, and helium, for which the thermal conductivity is known with considerable accuracy [15]. These calibrations were performed at pressures of 1 MPa for argon, 5 MPa for neon, and 10 MPa for helium, i.e., at pressures for which any temperature jump can be neglected [14].

The convection which takes place in the cell is assumed to be laminar. In that case, the correction for convection heat flow Q_c is approximated by the relation [16]

$$Q_c = \text{Ra} \frac{2\pi r}{720} \lambda \Delta T \quad (1)$$

where Ra is the Rayleigh number, λ is the thermal conductivity of the fluid, r is the radius of the inner cylinder, and ΔT is the temperature difference between the cylinders.

The measurements were not made at pressures lower than 1 MPa. Under this condition, the temperature-jump effect can be neglected.

3. RESULTS

The experimental data are presented in Table AI (Appendix). The thermal conductivity was determined with a reproducibility of 1% and an estimated accuracy of about 2% except in the critical region, where a reliable estimate of the accuracy is more difficult to make.

The density ρ was calculated from the equation of state developed by the National Bureau of Standard (Boulder) [17]. In this equation the critical parameters are the following:

$$T_c = 369.85 \text{ K}; \quad P_c = 4.2471 \text{ MPa}; \quad \rho_c = 220.5 \text{ kg} \cdot \text{m}^{-3}$$

The experimental data are shown in Fig. 1 as a function of the density along quasi-isotherms.

We have restricted the comparison of our data with the tabulated values proposed by Vargaftik et al. [6] and the correlation proposed by Holland et al. [7]. This comparison is shown in Fig. 2 for 0.1- and 30-MPa isobars. The experimental values at 0.1 MPa have been obtained by

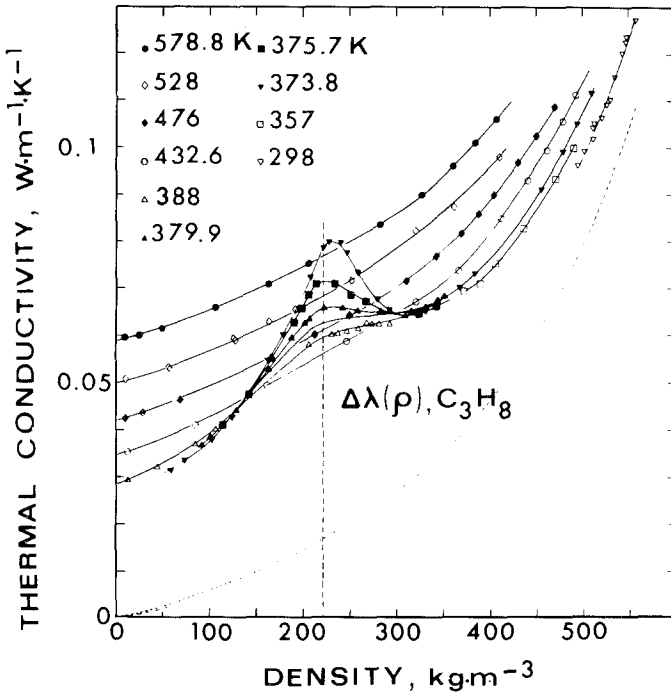


Fig. 1. The thermal conductivity of propane as a function of density and temperature.

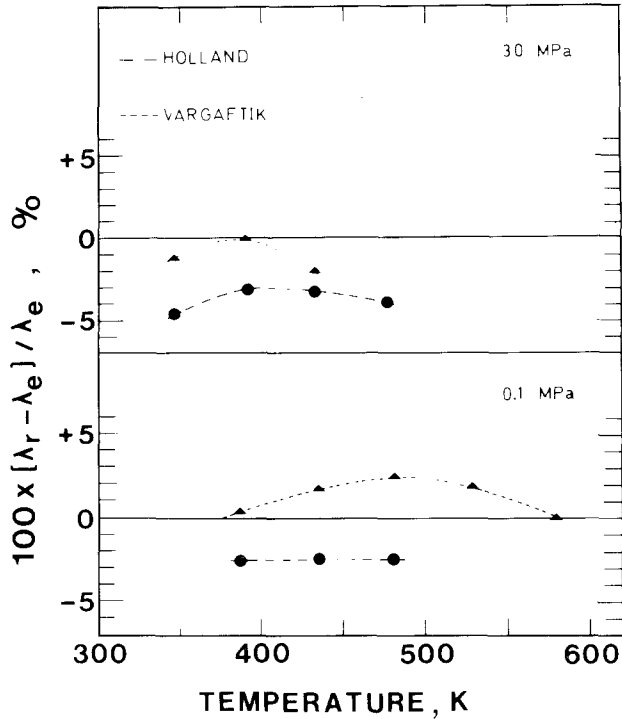


Fig. 2. Comparison between our experimental values of the thermal conductivity of propane at 0.1 MPa (extrapolated) and 30 MPa and the proposed values in Refs. 6 and 7.

extrapolation. It appears that our experimental values are in better agreement with the tabulated values proposed by Vargaftik et al.

We have presented in Fig. 3 the critical enhancement $\Delta\lambda_c(\rho, T)$ of the thermal conductivity of propane and in Fig. 4 the behavior of the critical enhancement at $\rho = \rho_c$ as a function of the temperature distance from the critical temperature.

$$\Delta\lambda_c(\rho, T) = \lambda(\rho, T) - \lambda_B(\rho, T) \quad (2)$$

with

$$\lambda_B(\rho, T) = \lambda_0(T) + \Delta\lambda(\rho) \quad (3)$$

$\lambda_0(T)$ is the dilute-gas thermal conductivity and $\Delta\lambda(\rho)$ is the "normal" density effect, which has been deduced from the behavior of the thermal conductivity far away from the critical point.

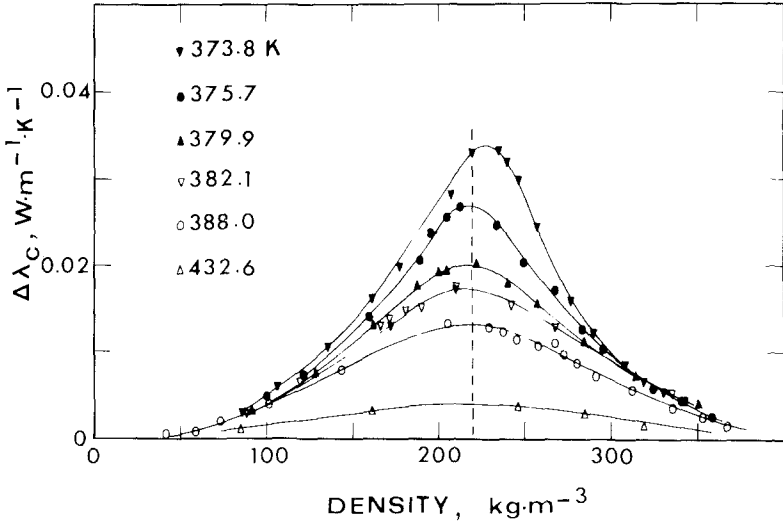


Fig. 3. The propane thermal conductivity critical enhancement.

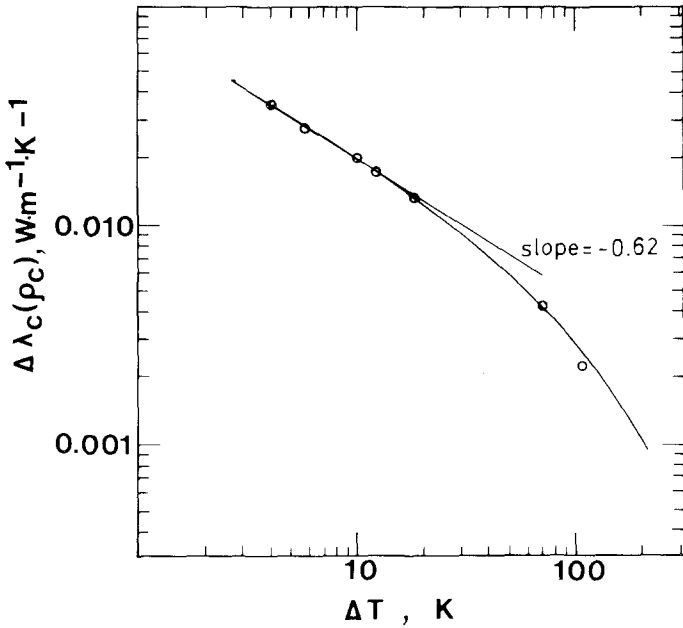


Fig. 4. The critical enhancement of the thermal conductivity of propane for the critical density as a function of the temperature difference ΔT ($\Delta T = T - T_c$).

$\lambda_0(T)$ can be represented by

$$\lambda_0(T) = \sum_{i=0}^4 A_i T^i \quad (4)$$

with $A_0 = 0.0242964$, $A_1 = -3.02775 \times 10^{-4}$, $A_2 = 1.58466 \times 10^{-6}$, $A_3 = -2.66226 \times 10^{-9}$, and $A_4 = 1.73834 \times 10^{-12}$. T is in K, and λ_0 in $\text{W} \cdot \text{m}^{-1} \cdot \text{K}^{-1}$.

$\Delta\lambda(\rho)$ can be written

$$\Delta\lambda(\rho) = \sum_{j=1}^5 B_j \rho^j \quad (5)$$

with $B_1 = 4.13863 \times 10^{-5}$, $B_2 = 2.47025 \times 10^{-7}$, $B_3 = -6.58197 \times 10^{-10}$, $B_4 = 1.29066 \times 10^{-12}$, and $B_5 = -4.25454 \times 10^{-17}$. ρ is in $\text{kg} \cdot \text{m}^{-3}$, and λ in $\text{W} \cdot \text{m}^{-1} \cdot \text{K}^{-1}$.

Figure 3 shows that the maximum of $\Delta\lambda_c(\rho_c)_T$ occurs at $\rho = \rho_c$ except for the 373.8 K isotherm, for which the maximum is located at $\rho > \rho_c$. Error bars on P , T , and eventually the equation of state (nonscaled equation of state in the critical region) can explain this shift. A small systematic error on P or T along this quasi-isotherm can also be possible.

The critical thermal conductivity excess along the critical isochore can be written [18]

$$\Delta\lambda_c = R \frac{k_B T}{6\pi\eta\xi} \rho_c C_p^c \exp(-At^2) \quad (6)$$

where R and A are adjustable constants, k_B is the Boltzmann constant, η is the shear viscosity, ξ is the long-range correlation length, C_p^c is the critical part of the specific heat at constant pressure, and $t = (T - T_c)/T_c$ is the reduced temperature distance from the critical temperature T_c .

Our data can be fitted with the following values of the parameters:

$$R = 1.2 \quad (7)$$

$$\xi = \xi_0 t^{-\nu} (1 + a_\xi t^4)$$

with $\xi_0 = 1.934 \text{ \AA}$, $a_\xi = 1.083$, $\nu = 0.63$, and $A = 0.5$;

$$C_p^c = \frac{T}{\rho_c} \left(\frac{dP}{dT} \right)_{\rho_c}^2 K_T \quad (8)$$

with $(dP/dT)_{\rho_c} = 7.8 \cdot 10^4 \text{ Pa} \cdot \text{K}^{-1}$; and

$$K_T = K_T^0 t^{-\gamma} (1 + a_x t^4) \quad (9)$$

where $K_T^0 = 1.1586 \cdot 10^{-8} \text{ Pa}^{-1}$, $a_x = 1.68$, and $\gamma = 1.24$.

$$A = 18$$

η is calculated using Eqs. (1), (3), (4), and (7) of Ref. 7.

K_7^o , a_x , ξ_o , and a_ξ have been estimated from the reduced compressibility and the reduced correlation length analysis proposed by Garabos [19, 20].

4. CONCLUSION

In this paper we have presented new results on the thermal conductivity of propane mainly at temperatures greater than the critical temperature over a wide density range. The present data should help in making data correlation with a greater accuracy, especially in the critical region.

APPENDIX

Table AI. Thermal Conductivity of Propane

T (K)	P (MPa)	ρ ($\text{kg} \cdot \text{m}^{-3}$)	λ ($\text{mW} \cdot \text{m}^{-1} \cdot \text{K}^{-1}$)
302.9 ₀	0.83	17.0	21.3
300.5 ₈	0.88	18.4	22.7
300.5 ₇	0.91	19.2	22.9
297.8 ₀	1.38	494.4	96.3
297.2 ₇	3.70	501.8	99.2
297.0 ₆	7.25	510.7	104.2
296.7 ₁	7.20	511.1	104.7
298.4 ₄	8.70	512.1	101.8
298.2 ₉	12.3	520.2	106.4
298.0 ₄	15.5	525.7	108.9
297.8 ₅	18.1	530.2	110.2
296.8 ₁	21.2	536.1	115.1
296.4 ₇	25.4	542.4	120.2
296.1 ₈	27.9	546.0	122.2
295.9 ₅	27.9	546.2	123.4
298.0 ₈	35.8	553.7	126.9
298.0 ₂	38.8	558.4	127.0
357.3 ₈	4.03	372.3	69.8
356.9 ₆	5.20	390.6	70.8
356.8 ₁	6.75	406.2	75.5
357.1 ₀	11.40	434.4	84.8
357.2 ₅	21.3	468.8	93.4
356.3 ₅	29.8	489.3	99.7
374.8 ₅	3.02	60.2	31.8
374.6 ₃	3.41 ₅	74.0	33.9

Table AI. (Continued)

T (K)	P (MPa)	ρ ($\text{kg} \cdot \text{m}^{-3}$)	λ ($\text{mW} \cdot \text{m}^{-1} \cdot \text{K}^{-1}$)
374.4 ₅	3.98	102.1	38.0
374.3 ₆	4.03	105.7	40.2
374.2 ₇	4.26	126.4	43.0
373.9 ₆	4.32	135.9	47.2
373.9 ₂	4.44 ₅	161.8	55.0
373.8 ₂	4.48 ₅	178.7	60.1
373.7 ₉	4.53 ₅	208.3	71.6
373.8 ₁	4.55 ₅	219.9	77.8
373.8 ₁	4.56 ₅	225.7	78.6
373.8 ₀	4.58 ₅	236.8	79.8
373.8 ₃	4.59 ₅	240.4	79.2
373.8 ₄	4.61	246.9	77.6
373.8 ₆	4.64	257.8	73.6
373.9 ₀	4.73	278.3	67.6
373.9 ₀	4.83	291.1	65.6
373.9 ₈	5.04	308.8	64.4
373.9 ₉	5.24 ₅	319.8	64.4
374.0 ₂	5.54	331.2	65.0
373.9 ₉	5.95	343.0	66.3
376.0 ₅	3.99 ₅	100.1	38.7
375.9 ₄	4.29	122.7	42.9
375.8 ₇	4.54 ₅	160.1	53.0
375.7 ₉	4.63 ₅	190.0	62.3
375.7 ₁	4.64 ₅	196.1	66.0
375.6 ₉	4.66 ₅	204.9	68.6
375.6 ₉	4.68 ₅	213.5	70.9
375.6 ₇	4.73 ₅	233.9	70.9
375.5 ₇	4.77 ₅	249.8	68.4
375.3 ₁	4.83	268.1	67.6
375.3 ₃	4.93	283.8	65.1
375.1 ₇	5.04	297.2	64.7
375.2 ₁	5.55	324.8	64.7
375.0 ₉	6.07	341.1	66.1
375.0 ₉	6.91	357.9	67.5
380.3 ₄	3.96 ₅	91.9	37.0
380.2 ₀	4.52 ₅	128.5	44.4
380.0 ₉	4.78 ₅	162.4	52.8
379.9 ₄	4.90	187.6	59.6
379.8 ₉	4.95	200.6	62.6
379.8 ₀	4.96 ₅	205.9	63.3
379.8 ₄	5.04	223.2	66.0
379.9 ₃	5.13 ₅	241.0	65.6
379.9 ₈	5.24 ₅	258.9	65.3
380.0 ₈	5.51	286.3	64.7

Table A1. (Continued)

T (K)	P (MPa)	ρ ($\text{kg} \cdot \text{m}^{-3}$)	λ ($\text{mW} \cdot \text{m}^{-1} \cdot \text{K}^{-1}$)
380.2 ₁	6.06	315.4	65.1
380.2 ₈	6.55 ₅	331.0	66.1
380.3 ₄	7.07	342.7	67.6
380.3 ₄	7.52	351.0	68.3
382.3 ₄	3.93 ₅	88.2	36.5
382.1 ₂	4.48 ₅	119.0	42.6
382.0 ₇	4.92	166.4	53.4
383.4 ₂	5.03	171.7	53.7
383.4 ₅	5.03	171.4	54.7
382.0 ₂	5.00	181.1	56.5
382.0 ₆	5.05	190.5	57.5
382.0 ₇	5.15 ₅	210.7	62.3
381.8 ₀	5.13 ₅	210.6	61.7
382.2 ₀	5.34 ₅	242.8	63.5
382.3 ₁	5.56	268.2	64.3
382.4 ₇	6.04 ₅	301.1	65.0
382.5 ₆	7.09 ₅	334.8	66.8
382.5 ₉	7.97 ₅	351.4	68.6
386.7 ₀	4.50 ₅	110.0	39.9
386.4 ₆	4.52 ₅	111.6	40.3
386.1 ₉	5.22 ₅	176.4	53.3
386.1 ₅	5.56 ₅	225.5	60.6
386.1 ₅	6.07 ₅	276.0	62.6
386.4 ₁	11.90	384.8	73.6
386.1 ₇	0.99	14.6	29.3
387.3 ₁	0.99	14.6	29.8
386.2 ₃	2.52	43.3	31.6
388.6 ₉	2.51	42.6	32.2
388.3 ₁	4.02	85.5	37.7
388.0 ₉	5.04	144.2	47.1
388.0 ₂	5.56	205.8	58.4
388.0 ₃	5.75 ₅	230.0	60.4
388.0 ₆	5.82 ₅	237.6	60.7
388.0 ₆	5.90 ₅	246.0	60.7
388.0 ₅	5.92	247.3	61.1
388.0 ₅	6.05 ₅	259.3	61.6
387.9 ₄	6.15 ₅	268.1	63.1
387.9 ₄	6.24	274.0	62.6
387.9 ₆	6.36	281.1	62.6
387.9 ₆	6.56	291.8	62.6
387.7 ₅	7.09	313.0	64.3
387.8 ₂	8.09	336.8	66.2
387.8 ₉	9.09 ₅	352.7	68.2
387.9 ₇	10.33	367.3	70.3

Table AI. (Continued)

T (K)	P (MPa)	ρ ($\text{kg} \cdot \text{m}^{-3}$)	λ ($\text{mW} \cdot \text{m}^{-1} \cdot \text{K}^{-1}$)
388.8 ₉	30.0	455.4	90.7
389.3 ₈	40.0	477.9	98.8
389.2 ₃	50.0	495.0	105.1
389.2 ₈	60.0	509.0	111.7
433.9 ₁	0.99	12.7	35.7
433.5 ₁	2.51	35.2	37.2
433.5 ₇	5.06	85.2	41.1
432.8 ₂	5.03	84.8	41.2
432.6 ₅	7.58	161.4	49.7
431.8 ₃	10.11	248.0	59.2
432.5 ₁	10.11	245.8	58.8
432.6 ₄	11.93	285.1	63.0
432.7 ₂	14.40	319.8	67.1
432.2 ₉	20.0	366.5	73.8
432.3 ₀	30.0	411.6	85.1
432.3 ₁	40.0	440.0	93.0
432.2 ₈	50.0	461.2	99.4
432.2 ₅	60.0	478.2	105.6
432.2 ₆	70.0	492.4	111.1
432.2 ₉	81.2	506.0	116.0
480.6 ₇	0.99	11.3	42.5
480.0 ₇	2.35 ₅	28.3	43.7
479.6 ₉	5.05	67.7	46.5
479.2 ₃	10.15	164.5	55.4
479.1 ₉	12.59	212.4	60.3
476.3 ₁	14.50	247.8	64.2
476.0 ₀	15.2	258.1	65.3
475.8 ₆	20.0	308.9	71.7
475.8 ₃	20.1	309.8	71.6
475.8 ₆	25.0	343.1	76.9
475.7 ₄	30.0	368.0	81.6
476.2 ₄	30.0	367.5	80.9
475.6 ₆	35.0	387.3	86.0
475.4 ₈	40.0	403.4	89.5
474.9 ₄	50.2	429.6	97.0
474.6 ₉	60.0	449.1	102.5
474.5 ₄	71.9	468.3	108.5
528.0 ₇	0.98	10.1	50.6
527.9 ₉	2.50	26.7	51.4
527.7 ₅	5.03	57.2	53.2
527.5 ₀	5.03	57.2	52.8
528.0 ₂	5.03	57.2	53.7
528.6 ₄	10.0	125.2	59.5
527.5 ₀	10.12	127.5	59.0

Table AI. (Continued)

T (K)	P (MPa)	ρ ($\text{kg} \cdot \text{m}^{-3}$)	λ ($\text{mW} \cdot \text{m}^{-1} \cdot \text{K}^{-1}$)
527.3 ₃	12.57	163.1	62.8
529.0 ₆	14.7	190.8	65.4
528.7 ₆	20.0	250.4	71.7
528.8 ₀	30.0	319.7	82.5
528.6 ₈	40.0	361.7	86.8
527.9 ₅	50.0	392.0	93.9
527.7 ₉	57.6	410.0	98.1
579.1 ₅	1.00	9.3	59.5
579.0 ₈	2.50	23.9	60.0
578.9 ₃	5.05	50.1	61.3
579.2 ₄	10.0	104.9	65.7
578.9 ₀	15.0	160.8	70.7
578.8 ₆	19.4	204.7	75.3
578.2 ₅	30.0	281.6	83.8
578.1 ₇	40.0	327.6	90.1
578.1 ₆	50.0	360.3	96.1
578.1 ₅	60.0	385.7	101.1
578.2 ₁	70.6	407.5	105.9

REFERENCES

1. D. E. Leng and E. W. Comings, *Ind. Eng. Chem.* **49**:2042 (1957).
2. N. I. Ryabtsev and V. A. Kazaryan, *Gazov. Prom.* **14**:46 (1969).
3. L. T. Carmichael, J. Jacobs, and B. H. Sage, *J. Chem. Eng. Data* **13**:40 (1966).
4. V. P. Brykov, G. Kh. Mukhamedzyanov, and A. G. Usmanov, *J. Eng. Phys. (USSR)* **18**:62 (1970).
5. H. M. Roder and C. A. Nieto de Castro, *J. Chem. Eng. Data* **27**:12 (1982).
6. N. B. Vargaftik, L. P. Filippov, A. A. Tarzimanov, and E. E. Totskin, in *Teploprovodnost Jidkosti i Gazov* (Izdatelstvo Standartov, Moskva, 1978).
7. P. M. Holland, H. J. M. Hanley, K. E. Gubbins, and J. M. Haile, *J. Phys. Chem. Ref. Data* **8**:559 (1979).
8. R. Tufeu, B. Le Neindre, and P. Bury, *Physica* **44**:81 (1969).
9. B. Le Neindre, R. Tufeu, P. Bury, P. Johannin, and B. Vodar, in *Thermal Conductivity 8th*, C. Y. Ho and R. E. Taylor, eds. (Plenum Press, New York, 1969).
10. R. Tufeu, Y. Garrabos, and B. Le Neindre, in *Thermal Conductivity 16*, D. C. Larsen, ed. (Plenum Press, New York, p. 605).
11. C. A. Nieto de Castro, R. Tufeu, and B. Le Neindre, *Int. J. Thermophys.* **4**:11 (1983).
12. J. C. Nieuwoudt, B. Le Neindre, R. Tufeu, and J. V. Sengers, *J. Chem. Eng. Data* (in press).
13. B. Le Neindre, Thesis (Université Paris VI, Paris, 1969).
14. R. Tufeu, Thesis (Université Paris VI, Paris, 1971).
15. J. Kestin, R. Paul, A. A. Clifford, and W. A. Wakeham, *Physica* **100** A:349 (1980).
16. P. Johannin, Thesis (Université Paris, Paris, 1958).

17. B. A. Younglove, NBS Technical Note 1048, NBS U.S. Department of Commerce, Washington, D.C. (1982); R. D. Goodwin and W. N. Haynes, NBS Monograph 170, NBS U.S. Department of Commerce, Washington, D.C. (1982).
18. H. J. M. Hanley, J. V. Sengers, and J. F. Ely, in *Thermal Conductivity 14*, P. G. Klemens and T. K. Chu, eds. (Plenum, New York, 1976), p. 383.
19. Y. Garrabos, *J. Phys. (Paris)* **46**:281 (1985).
20. Y. Garrabos, *J. Phys. (Paris)* **47**:111 (1986).